

An Approximate Analysis for Hertzian Elliptical Wheel-Rail Contact Problem

Jay Prakash Srivastava
Department of Mechanical Engineering
Indian School of Mines
Dhanbad, India
jaysrvstv@gmail.com

P.K. Sarkar¹, Vinayak Ranjan²
Department of Mechanical Engineering
Indian School of Mines
Dhanbad, India
¹sarkarpk1955@yahoo.co.in
²vinayakranjan@yahoo.com

Abstract— The wheel-rail contact condition is modeled assuming two general quadratic surfaces. The formulation in this study aims primarily at determination of stresses by varying contact geometry arising from variation in profile geometry. A change in surface topology, may result from wear, brings in a change in contact geometry and stresses. To understand their influence profile radii are changed for six different values. Problem formulation is based on Timoshenko's approach. Correspondingly, variations in the results in terms of principal stresses with changes in wheel profile radii, wheel taper and rail profile radii are obtained. A comparison with available published results shows an error within two to three percent of models [1, 2]. Results obtained are expected to help understand the rail wheel topology dependence on the stress deformation pattern. This may allow a direct design application for railways in particular.

Keywords— *Hertz Contact, Wheel-Rail, Contact Dimensions, Contact profile, Contact Stress, Contact Pressure, Radius of Curvatures.*

I. INTRODUCTION

Rail wheel contact phenomena results in stick slip wear, giving rise to crack initiation and its propagation to yield catastrophe. The contact condition in terms of contact pressure and sliding velocity are found to be more important than the grade of steel [3]. Assessment of contact stresses at the wheel-rail interface thus poses a very important issue in a study of rail-wheel contact phenomena. It is important to understand here that rail-wheel contact pair's profile radii change with time and wear. This has drawn much attention of many researchers to investigate the problem mainly by means of theoretical or numerical approaches for the solution of Hertz theory [4]. Hertz contact theory appeared in 1881 to solve the problem of pressure distribution between two elastic spherical bodies in contact. Later he extended it to general case of two elastic bodies in contact. Then onwards researchers have used this theory for the analysis of the wheel-rail contact problem numerically to reach a more realistic solution. A practical and accurate formulation is still in demand [2]. The contact-pair topology influences the contact stress magnitude and shape of contact area. To speed up the process of calculation and accurate the model, Fischer et. al [1] proposed a solution for contact dimension, contact pressure and penetration. They

considered variation in profile geometry in evolving their formulas. They applied regression analysis to eliminate calculation of elliptic integrals to find their contact geometry relation to reveal the consequence of topology variation on contact pressure. At wheel-rail contact, Hertz equation can only be applied at the contact between wheel and rail head [2], however, not at the contact between wheel flange and gage corner since the radius of the contact body is smaller than the radius of contact area [5]. Brewe et. al [6] determined an approximate equation to obtain value for elliptical semi axes. Hamrock [7] reinvestigated Hertz problem to obtain a new approximate equation for elliptical axis ratio and elliptic integral. Greenwood [8] introduced effective radius method for the Hertz pressure. Later on Tanaka [9] established a new method to calculate elliptical (Hertz) contact pressure wherein the calculation of elliptical integral is not necessary. Subsequently, Antonie et. al [10] obtained an approximate solution of Hertzian contact model by replacing the elliptical integral with polynomial approximation. Hanson et. al [11] extended Hertz theory to the elastic field expression for the transversely isotropic body with ellipsoidal variation of normal traction and shear traction loading on the surface. Liu et. al [12] found an expression to calculate Hertzian contact elliptic dimensions and contact pressure for the coated bodies for contact characteristics. Present study utilizes the application of hertz contact theory to the wheel-rail contact problem to study the effect of variation of wheel rail profile parameters on the contact dimension and contact stresses. In contact zone between wheel and rail, normal and tangential loads are transmitted. The way steel wheel meets the steel rail and size of the forces transmitted into contact zone influence various damage mechanisms like, wear and surface cracking. The wheel load is transmitted to the rail through a tiny contact area under high contact stress. This results in repeated loading above the elastic limit which leads to plastic deformation. The depth of plastic flow depends on the hardness of the rail and the severity of the curves.

II. MATHEMATICAL MODEL FOR WHEEL-RAIL CONTACT

First, According to Yan [13], if two elastic nonconforming bodies are pressed together then the contact area assumes elliptical shape with a semi major

axis 'a' and a semi minor axis 'b'. The distribution of the contact pressure in this elliptical area as shown in Fig. 1 represents a semi-ellipsoid, expressed [14] as:

$$P = P_o \left(1 - \frac{x^2}{a^2} - \frac{y^2}{b^2}\right) \quad (1)$$

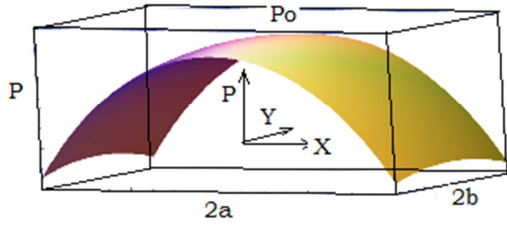


Fig. 1: Pressure distribution across elliptic area

The method assumes the contact surfaces to be smooth, so they can be described by a second-degree polynomial

$$Z_1 = A_1x^2 + A_2xy + A_3y^2 \quad (2)$$

$$Z_2 = B_1x^2 + B_2xy + B_3y^2 \quad (3)$$

Parameters in above Eqs. 2, 3 are represented in Fig. 2.

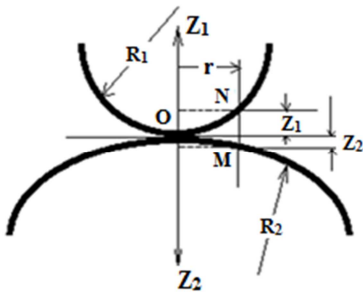


Fig. 2: General Profiles of two contacting bodies

The contact plane is held immovable during compression. Any two points of the contacting bodies on the axes Z_1 and Z_2 at large distances from O will approach each other differing by a certain amount α , and the distance between two points such as M and N will diminish by $\alpha - (w_1 + w_2)$. From geometrical consideration it can be written as

$$w_1 + w_2 = \alpha - (Z_1 + Z_2) \quad (4)$$

Where, w_1 and w_2 denote the displacement of a point due to the local deformation in the Z direction respectively. Using Boussinesq's [15] solution for a semi-infinite body subjected to a concentrated normal force at the boundary surface displacement w_1 and w_2 is given by:

$$w_1 = K_1 \iint p \, d\Psi \, ds \quad (5)$$

$$w_2 = K_2 \iint p \, d\Psi \, ds \quad (6)$$

K_1 and K_2 are constants given by $K_1 = \frac{1-\mu_1^2}{\pi E_1}$ and $K_2 = \frac{1-\mu_2^2}{\pi E_2}$, μ & E are elastic constants. Substitution of Eqs. (2), (3), (5) and (6) in Eq. (4) provides:

$$(K_1 + K_2) \iint \frac{p \, dA}{r} = \alpha - Ax^2 - By^2 \quad (7)$$

The distribution of pressure P is found by assuming the intensity of pressure over the surface of contact to be represented by the ordinates of a semi-ellipsoid constructed on the surface of contact [16]. The maximum pressure is obtained by satisfying roots of the Eq. (7), occurs at the center of the surface of contact is given by [17]:

$$P_o = \frac{3}{2} \frac{P}{\pi ab} \quad (8)$$

The semi axes of the elliptic boundary of the surface of contact 'a', 'b' are given by [18]:

$$a = m \left[\frac{3\pi P(K_1 + K_2)}{4(A+B)} \right]^{1/3} \quad (9)$$

$$b = n \left[\frac{3\pi P(K_1 + K_2)}{4(A+B)} \right]^{1/3} \quad (10)$$

The calculation of the contact areas requires knowledge of some geometric constants used in the above formulation. With respect to wheel-rail configuration, the following curvature combinations are related as:

$$A + B = \frac{1}{2} \left(\frac{1}{R_{11}} + \frac{1}{R_{12}} + \frac{1}{R_{22}} + \frac{1}{R_{21}} \right) \quad (11)$$

$$B - A = \frac{1}{2} \left[\left(\frac{1}{R_{11}} - \frac{1}{R_{12}} \right)^2 + \left(\frac{1}{R_{22}} - \frac{1}{R_{21}} \right)^2 + 2 \left(\frac{1}{R_{11}} - \frac{1}{R_{12}} \right) \left(\frac{1}{R_{22}} - \frac{1}{R_{21}} \right) \cos 2\psi \right]^{1/2} \quad (12)$$

Where A and B are positive constants. R_{11} , R_{12} , R_{21} and R_{22} are defined as the principal relative radii of curvature, represented pictorially in the Fig. 3.

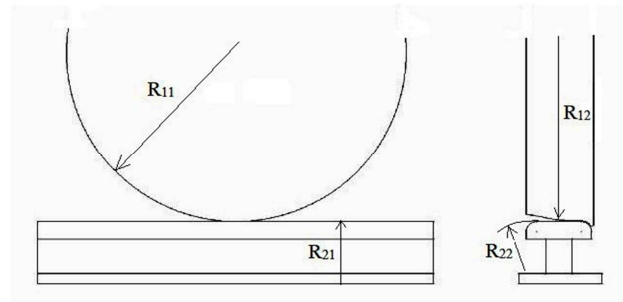


Fig. 3: Wheel-Rail Configuration showing different principal relative radii of curvature

Where,

R_{11} : The rolling radius of curvature of the wheel.

R_{12} : The radius of the wheel profile, which goes to infinity for a conical wheel.

R_{21} : The radius of the runway which is infinity in this case.

R_{22} : The radius of curvature of the rail in the plane of cross section.

The ellipticity parameter $\left(\frac{a}{b}\right)$ is related to geometrical parameter $\left(\frac{A}{B}\right)$ by means of the coefficients 'm' and 'n'. From the notation, $\cos \theta = \frac{B-A}{A+B}$ the values of m and n for various values of θ are calculated using the Table [19]. By means of best curve fitting method shown in Fig. 4 and Fig. 5 the intermediate values are calculated using regression given by:

$$n = 3E-05\theta^2 + 0.0045\theta + 0.334 \quad (13)$$

$$m = 62.19\theta^{-0.914} \quad (14)$$

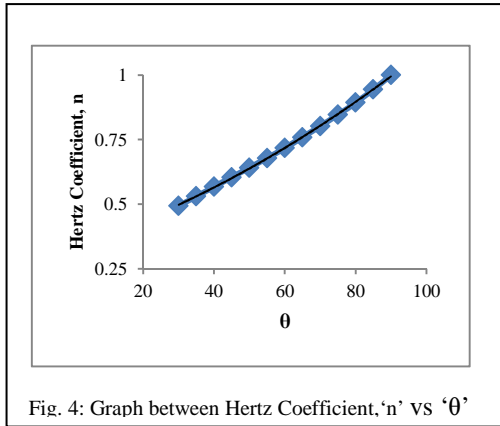


Fig. 4: Graph between Hertz Coefficient, 'n' vs 'theta'

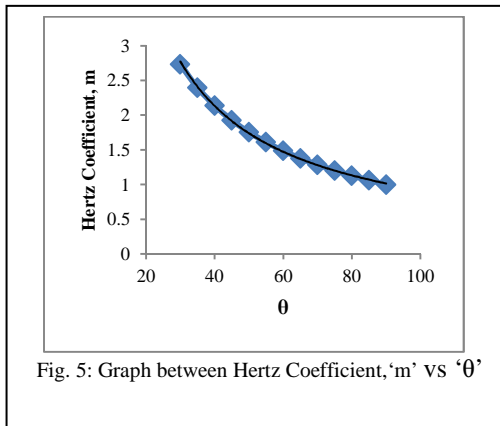


Fig. 5: Graph between Hertz Coefficient, 'm' vs 'theta'

The principal stresses at the centre of the surface of contact are calculated as [13]:

$$\sigma_1 = -2\mu P_0 - (1 - 2\mu)P_0 \frac{b}{a+b} \quad (15)$$

$$\sigma_2 = -2\mu P_0 - (1 - 2\mu)P_0 \frac{a}{a+b} \quad (16)$$

$$\sigma_3 = -P_0 \quad (17)$$

Evaluated results are presented in Tables [1-3].

III. RESULTS

The above Eqs. (8-17) are used to calculate the contact dimension & contact pressure between wheel-rail contact pair varying contact geometry. The wheel and rail used in the present study is as per Indian Railway standards [20].



Fig. 6: Wheel Profile as per Indian railway standard

The variations in the geometrical parameter considered are wheel taper from 1 in 5 to 1 in 30, wheel profile radius from 300 to 360 mm and rail profile radius from 280 to 330 mm. The material model is linear-elastic and there is no friction between the contacting surfaces. The contact load is taken as 10 tonne. Material data $E_{\text{wheel}}=210$ GPa, $E_{\text{rail}}=200$ GPa, $\mu_{\text{wheel \& rail}}=0.3$, $\sigma_{\text{ut}}^{\text{rail}} = 680$ MPa, $\sigma_{\text{ut}}^{\text{wheel}} = 883$ MPa, $\sigma_y = 0.5 \sigma_{\text{ut}}$ for both, are used for the pair of contacting bodies.

Table 1: Effect of variation in Wheel Profile Taper (WPT) on different contact parameters, $R_{11}=1098$ mm, $R_{12}=330$ mm, $R_{21}=\infty$, $R_{22}=300$ mm

WPT	a (mm)	b (mm)	P_0 (MPa)	σ_1 (MPa)	σ_2 (MPa)	σ_3 (MPa)
1 in 5	11.4	3.27	1258.7	-867.9	-1146.1	-1258.7
1 in 10	11.6	3.24	1248.3	-858.1	-1139.2	-1248.3
1 in 15	11.6	3.23	1246.2	-856.2	-1137.8	-1246.2
1 in 20	11.6	3.23	1245.5	-855.5	-1137.3	-1245.5
1 in 25	11.7	3.23	1245.2	-855.5	-1137.3	-1245.2
1 in 30	11.7	3.23	1244.9	-855.5	-1136.9	-1244.9

Table 2: Effect of variation of radius of curvatures of wheel profile on contact parameters, Wheel profile Taper (WPT) =1in 20, ϵ (deg) = 2.86, $R_{11} =1098$ mm, $R_{21}=\infty$, $R_{22}=300$ mm.

R_{12} (mm)	a (mm)	b (mm)	P_0 (MPa)	σ_1 (MPa)	σ_2 (MPa)	σ_3 (MPa)
300	11.7	3.15	1268.8	-868.9	-1161.1	-1268.8
310	11.7	3.18	1260.7	-864.2	-1152.8	-1260.6
320	11.7	3.21	1252.9	-859.8	-1144.8	-1252.9
330	11.6	3.23	1245.5	-855.5	-1137.3	-1245.5
340	11.6	3.25	1238.5	-851.5	-1130.1	-1238.6
350	11.6	3.28	1231.9	-847.7	-1123.4	-1231.9
360	11.6	3.30	1225.5	-844.1	-1116.9	-1225.5

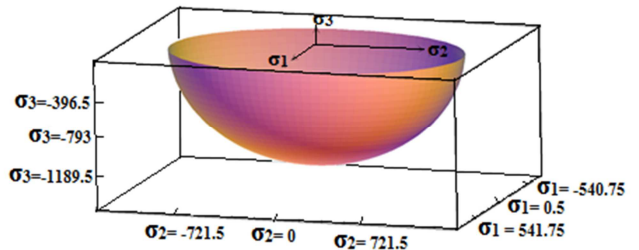


Fig. 7: A representative Stress Ellipsoid for $R_{12}=300$ mm, giving $\sigma_1 = -868.93$ MPa, $\sigma_2 = -1161.12$ MPa and $\sigma_3 = -1268.78$ MPa from Table -2.

Table 3: Effect of variation of radius of curvatures of rail profile on contact parameters, Wheel profile Taper (WTP) = 1 in 20, ϵ (deg) = 2.86, R_{11} = 1098 mm, R_{12} = 330 mm, R_{21} = ∞

R ₂₂ (mm)	a (mm)	b (mm)	P _o (MPa)	σ_1 (MPa)	σ_2 (MPa)	σ_3 (MPa)
280	11.7	3.17	1263.8	-866.0	-1156.1	-1263.8
290	11.7	3.20	1254.4	-860.6	-1146.4	-1254.4
300	11.6	3.23	1245.5	-855.5	-1137.3	-1245.5
310	11.6	3.26	1237.1	-850.7	-1128.7	-1237.1
320	11.6	3.29	1229.1	-846.1	-1120.5	-1229.1
330	11.6	3.31	1221.5	-841.7	-1112.8	-1221.6

Results from the present model are compared with those of [1] and [2]. Findings can be seen well in agreement. The accuracy in 'P_o' is in the range of 2-3%, in 'a' it is in the range of 2-3% and in 'b' it is in the range of 0-1%.

Table 4: Comparison of the obtained results from present formulae with those in [1] and [2].

R ₁₂ (mm)	Solution given by [1] (%)			Solution given by [2] (%)		
	a	b	P _o	a	b	P _o
300	2.74	0.07	-3.04	2.24	0.68	-3.07
310	2.94	0.16	-3.02	2.42	0.77	-3.04
320	3.13	0.29	-3.00	2.59	0.89	-3.00
330	2.42	0.13	-2.99	1.88	0.74	-2.98
340	2.59	0.00	-2.97	2.03	0.61	-2.94
350	2.76	0.21	-2.96	2.18	0.82	-2.92
360	2.91	0.14	-2.95	2.32	0.75	-2.90
R ₂₂ (mm)	Solution given by [1] (%)			Solution given by [2] (%)		
	a	b	P _o	a	b	P _o
280	2.85	0.19	-3.03	2.35	0.80	-3.05
290	3.08	0.14	-3.01	2.56	0.75	-3.01
300	2.42	0.13	-2.99	1.88	0.74	-2.97
310	2.63	0.15	-2.97	2.07	0.76	-2.94
320	2.83	0.21	-2.95	2.24	0.82	-2.90
330	3.02	0.00	-2.93	2.42	0.61	-2.87
WPT	Solution given by [1] (%)			Solution given by [2] (%)		
	a	b	P _o	a	b	P _o
1 in 5	-0.26	2.08	-1.33	0.12	2.30	-1.90
1 in 10	2.19	0.54	-2.63	1.88	1.05	-2.76
1 in 15	2.32	0.17	-2.87	1.88	0.74	-2.92
1 in 20	2.36	0.15	-2.96	1.88	0.74	-2.98
1 in 25	3.27	0.14	-2.99	2.76	0.74	-3.00
1 in 30	3.28	0.14	-3.02	2.76	0.74	-3.02

IV. DISCUSSION ON RESULTS

Table 1 presents the results showing effect of variation in wheel taper, designated by Ψ . Increase in contact length and decrement in contact width is observed with decrease in taper. Contact pressure and contact stress decreases with the decrease in wheel taper. Effect of variation in the radius of curvature of wheel profile on contact parameters is shown in Table 2. Increase in contact width and reduction in contact length is observed with the increase of radius of curvature. Contact pressure and contact stress shows reduction with increase in wheel profile radii. Similar trend is observed with varying the radii of curvatures of rail profile, tabulated in Table 3. This gives an indication of increasing sliding friction. Contact dimension and contact pressure results from the

present formulation are compared with the results in [1, 2]. Remarkably they are in close agreement. Percentage error in pressure estimation is within 2-3 %. The contact dimensions 'a' and 'b', estimated from the current model compares with those of [1, 2] in range of 0-3% in the case in 'a' and 0-2% in the case in 'b'. These Results are shown in Table 4. Fig. 7 depicts the contact stress distribution over the contact area in the form of a stress ellipsoid, shown as a representative case. This helps to better visualize the stress-contact geometry interaction.

V. CONCLUSION

Rail wheel contact problem varying contact profile geometries is investigated to estimate the influence of contact geometry and stress distribution. Results from the present model indicate stress decrement with increase in profile radii. Increase in wheel profile radii also increases width of the contact area ellipse while its length decreases. This is likely to induce higher sliding friction. Influence of taper increase, represented by Ψ , causes increase in contact length with reduced width. Thus, higher taper of rail wheel is likely to facilitate reduction in contact area. Contact stress results compared with models of [1, 2] can be seen to be in close agreement with an error in the range of 2-3%. Thus, the present analysis may help in rail wheel profile design keeping care of contact area, contact stress, contact geometry, and contact pressure in wheel. The stress-ellipsoids indicate the dependence of stress state on the contact pair topology. Better revelation is expected to be achieved from a finite element analysis. This investigation considers static contact condition as a preliminary to future study of their dynamic behavior.

REFERENCES

- [1] F. D. Fischer and M. Wiest, Approximate Analysis Model for Hertzian Elliptical Wheel/Rail or Wheel/Crossing contact Problems, ASME Journal of Tribology, 130, 2008, pp. 1-3.
- [2] S. Soemantri, W. Puja, B. Budiwantoro, M. Parwata, D. J. Schipper, Solution to Hertzian contact problem between Wheel and Rail for small radius of curvature, JSME, 4, 2010, pp. 669-677.
- [3] T. Matsudaira, Dynamics of High Speed Rolling Stock, Japanese National Railways RTRI Quarterly Reports, Special Issue, 1963.
- [4] H. Hertz, On The Contact of two Elastic Solids, London: Macmillan & Co. Cap. 5, 1896, pp. 146-162.
- [5] Y. Liu, L. Liu, S. Mahadevan, Analysis of subsurface crack propagation under rolling contact loading in railroad wheels using FEM, Engineering Fracture Mechanics, 74, 2007, pp. 2659-2674.
- [6] D. E. Brewe and B. J. Hamrock, Simplified solution for elliptical contact deformation between two elastic solids, ASME Journal of Lubrication Technology, 99, 1977, pp. 485-387.
- [7] B. J. Hamrock and D. E. Brewe, Simplified solution for stresses and deformations, ASME Journal of Lubrication Technology, 105, 1983, pp. 171-177.
- [8] J. A. Greenwood, Analysis of elliptical Hertzian. Tribology International, 30, 1997, pp. 235-237.
- [9] N. Tanaka, A new calculation method of Hertz Elliptical contact pressure, ASME Journal of tribology, 123, 2001, pp. 887-889.
- [10] J. F. Antoine, C. Visa, C. Sauvey, and G. Abba, Approximate Analytical model for Hertzian elliptical contact problems, ASME Journal of tribology, 128, 2006, pp. 660-664.
- [11] Mark T. Hanson and Gn. Wiratmaja Puja, The Elastic Field resulting from elliptical hertzian contact of transversely isotropic

- bodies: closed form solution for normal and shear loading, ASME Journal of Applied Mechanics 1996.
- [12] S. B. Liu, A. Peyronnel, Q. J. Wang and L. M. Keer, An extension of the Hertz theory for three-dimensional coated bodies, Tribology Letters, 18, 2005, pp. 303-314.
- [13] W. Yan, F.D. Fischer, Applicability of the Hertz Contact Theory to rail-Wheel contact problem, Archive of Applied Mechanics, 70, 2000, pp. 255-268.
- [14] K. L. Johnson, Contact Mechanics, Cambridge University Press, Cambridge, 1985, pp. 85-106.
- [15] J. Boussinesq, Application des Potentiels a l'etude de l'equilibre et du mouvement des solides elastiques, Gauthier-Villars, Paris, 1885.
- [16] S. P. Timoshenko, and J. N. Goodier, Theory of Elasticity, 3rd edition, McGraw-Hill Book Co. Inc., New York, 1970, pp. 409-416.
- [17] A. Anyakwo, C. Pislaru, A. Ball, A new method for modelling and simulation of the dynamic behaviour of the wheel-rail contact, International Journal of Automation and Computing, 9, 2012, pp. 237-247.
- [18] N. Zong, M. Dhanasekar, Analysis of Rail Ends under Wheel Contact Loading, International Journal of Mechanical and Aerospace Engineering, 6, 2012, pp. 452-460.
- [19] H. L. Whittemore, and S. N. Petrenko, Technical Paper 201. National Bureau of Standards, 1921.
- [20] Maintenance Manual for Wagon, Government of India, Ministry of Railways (Railway Board), March 2001.